STUDIES OF REACTION GEOMETRY IN OXIDATION AND REDUCTION OF THE ALKALINE SILVER ELECTRODE

SIXTH QUARTERLY REPORT

Eliot A. Butler

Angus U. Blackham

November 15, 1969

J. P. L. 952268

This work was performed for the Jet Propulsion Laboratory, California Institute of Technology, as sponsored by the National Aeronautics and Space Administration under Contract NAS7-100.

Brigham Young University

Provo, Utah

STUDIES OF REACTION GEOMETRY IN OXIDATION AND REDUCTION OF THE ALKALINE SILVER ELECTRODE

SIXTH QUARTERLY REPORT

Eliot A. Butler

Angus U. Blackham

November 15, 1969

J. P. L. 952268

Brigham Young University

Provo, Utah

This report contains information prepared by Brigham Young University under JPL sub-contract. Its content is not necessarily endorsed by the Jet Propulsion Laboratory, California Institute of Technology, or the National Aeronautics and Space Administration.

ABSTRACT

The design of the model pore electrode has been substantially changed. Bundles of seven and nineteen wires are tightly enclosed in channels of hexagonal cross section. Three electrodes of larger pore sizes have been constructed, and have been subjected to oxidation-reduction cycling at constant current. Characteristic features of potential response are discussed. Charge acceptance was found to be a function not only of surface area and current, but also of pore size. Whether the effect of the pore size results from changes in the electrical resistance in the pore or from changes in the electrolyte flow rate has not yet been determined. Surface characteristics of the electrode are described.

When silver wire electrodes were subjected to fixed controlled potentials, very rapid increases in current density were observed with an oscilloscope. Peak values were reached within 0.25 millisecond. The current densities decreased to about half of the peak values within 2.0 milliseconds. The charge accepted during the rise of current density to this peak value was approximately the same as that required to charge the double layer.[5] Therefore, the initial peak values of current density may be due principally to the charging of the double layer with almost no contribution coming from a faradaic current.

TABLE OF CONTENTS

SECTION I

OXIDATION OF MODEL PORE ELECTRODES

Introduction

Previous work on model pore electrodes of three sizes has shown: (1) that the extent of penetration into the pores by both silver (I) and silver (II) oxides decreases as the pore size decreases; and (2) that both oxide films penetrate the pore to a lesser extent as the flow rate of the electrolyte through the electrode is increased.[1]

In an effort to improve and expand our data we have significantly changed the design of the holder to obtain the closest possible packing of the wires. In addition, we have added to our inventory electrodes of three larger pore sizes.

Experimental

In the last quarterly report, the electrode then in use was illustrated in Figure 10.[1] The holder for the wires was a modified capillary tube. The cylindrical shape of the holder successfully effected a symmetric arrangement of the wires; and this yielded pores of uniform size. However, difficulties were encountered with electrodes composed of large numbers of small diameter wires. As can be seen in Figure 2a, the cross-section of seven wires forms a hexagon that fits a circle well. When the electrode is expanded to nineteen wires, another hexagon is obtained which has one wire on each side that does not touch the circle. Therefore, the fit is poor and there are six large spaces that the wires could

leave their hexagonal arrangement to fill. In practice this is what occurs, and it is accompanied by the loss of uniform pore size. It was observed that the most efficient arrangement of wires was hexagonal close pack, so we constructed a holder with a hexagonal hole. It is illustrated in Figure 1.

The hole (A) is made by milling each half of the 1/8" plexiglass with a shaped drill. Tolerances of ± 1.0 mil are obtained. A gasket is formed on both sides of the groove using silicone rubber sealer (Dow-Corning Corporation). The halves are then clamped together with four screws (C). Screw holes (D) are drilled and tapped in the top of the body to permit the attachment of the stem. Another silicone rubber gasket (E) is formed at the bottom of the stem. A short length of glass tubing (F) is inserted in a hole on the upper portion of the stem. It serves as an inlet for the electrolyte. A short length of tygon tubing (G) is used to join a 12 cm portion of 7 mm pyrex glass tubing (H) to the stem. The bundle of wires enclosed in the holder have been fused (I) to a lead wire (J) that passes through a septum cap (K).

After the electrode has been assembled, small portions of the silicone rubber are applied to: (1) the joint between the tygon tubing (G) and the stem; (2) the joint between the glass tubing (F) and the stem; and (3) the joint between the stem and the body. These were applied as further insurance against electrolyte leaks. This three-part design (two body halves and stem) was employed because of the difficulties encountered in

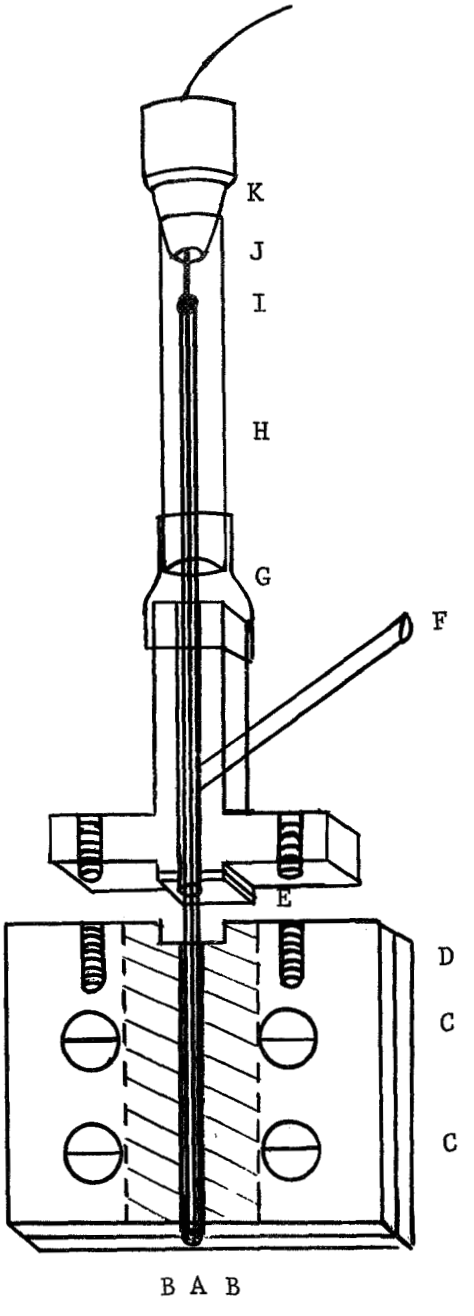

Fig. 1. -- Model pore electrode.

machining a hexagonal hole when the stem and body are one solid piece. Experiments with heated hex rod proved fruitless because the plexiglass contracts irreproducibly after the rod is removed.

The piece of glass tubing has been included to handle the increased length of the bundle of wires. The length was increased for two reasons: (1) to make it possible (having slid the glass back up the lead wire) to push the lower, oxidized portion of the wires out of the hole for microscopic examination; and (2) to avoid wasting the portion of the wires which resided in the stem and was unoxidized, but had to be discarded with the rest of the electrode when it required replacement.

The unfused tips of the wires were masked by pressing them against a thin layer of partially cured epoxy cement. After twenty minutes, the wires were individually stroked to insure that no cement extended beyond the edge of the tip. Before the wires were inserted into the holder, they were cleaned with a cleanser slurry and thoroughly rinsed.

Electrodes of larger pore sizes have been fabricated using 25 mil, 40 mil, and 51 mil diameter wires. Table I compares several dimensions of these electrodes. As indicated in the table, the hexagonal packing of wires created three types of pores. Figure 2 illustrates the geometry of these pores, the equations used in calculating their surface area contributions, and the geometry of hexagonal close packing in electrodes of two different sizes.

TABLE I

Dimensions of Three Model Pore Electrodes

ELECTRODE		A	B	C
Length of side (mm)		2.04	1.60	1.63
Wires	Number	7	7	19
	Size (mil)	51	40	25
	Radius (mm)	0.65	0.51	0.32
Number of Pores	Type 1	6	6	12
	Type 2	6	6	24
	Type 3	6	6	6
Cross Sectional Area (mm^2)	Electrode	10.8	6.65	6.90
	Wire	9.3	5.72	5.95
	Pore	1.5	0.93	0.95
Surface Area per mm into the pore	Wire	28.6	22.4	37.6
	Pore	40.8	32.0	47.5

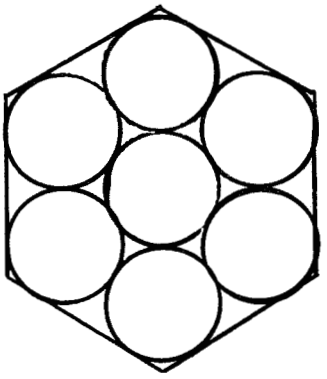

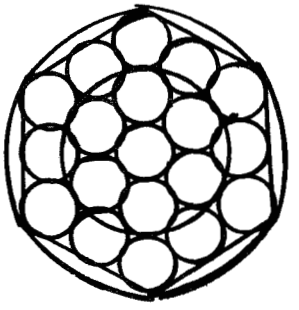

$$A_{hex} = 2.598\ L^2$$

(a)

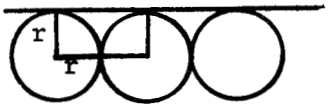

$$A_{pore} = 2r^2 - 2\,\frac{\pi r^2}{4}$$
$$= 0.429r^2$$

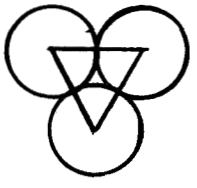

$$A_{pore} = \tfrac{1}{2}(2r)(2r\sin 60^\circ) - \tfrac{1}{2}\pi r^2$$
$$= 0.161r^2$$

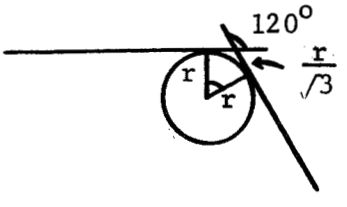

$$A_{pore} = \frac{1}{\sqrt{3}}\,r^2 - \frac{\pi}{6}\,r^2$$
$$= 0.053r^2$$

(b)

Fig. 2. -- Geometry of the model pores.

The following experimental procedure was used. A 0.1 F KOH solution was forced, by gravity flow, to pass into the arm (F) of the stem, through the holder, and into the reservoir containing a cylindrical platinum counter electrode. The reference electrode was a calomel type. The flow was kept constant during both oxidation and reduction. The electrode was cycled through oxidation and reduction while it was in the holder.

RESULTS AND DISCUSSION

The data obtained to date are preliminary but encouraging. Representative oxidation curves are illustrated in Figure 3. Approximately 5% of the curves had the shape of 3a, 65% had the shape of 3b, and 30% had the shape of 3c. Three points on curve 3b have been labeled. They are the points of significant changes of slope in the oxidation curve and have been determined for each curve wherever possible. P_3, for example, is the only point marked on curve 3a, and the only point absent from curve 3c. It is at this point in the oxidation that oxygen evolution is noted. The geometric method used to determine these points is illustrated in Figure 4.

Table II contains the potentials obtained during the oxidation of the three electrodes described in Table I. The reproducibility is good and the increase of potential with increasing applied current is as would be expected from overvoltage considerations. The electrodes are listed in order of increasing surface area per millimeter into the pore. Data are absent for electrode B at 1600 μA

Fig. 3. -- Representative oxidation curves.

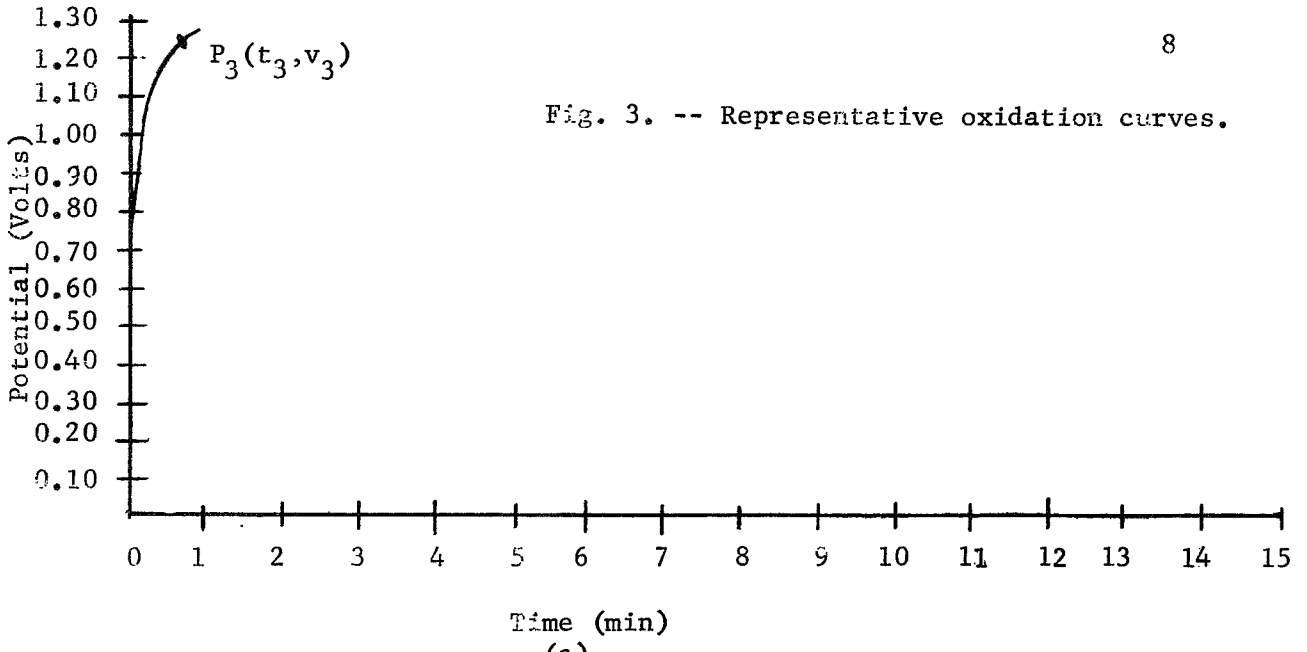

(a)

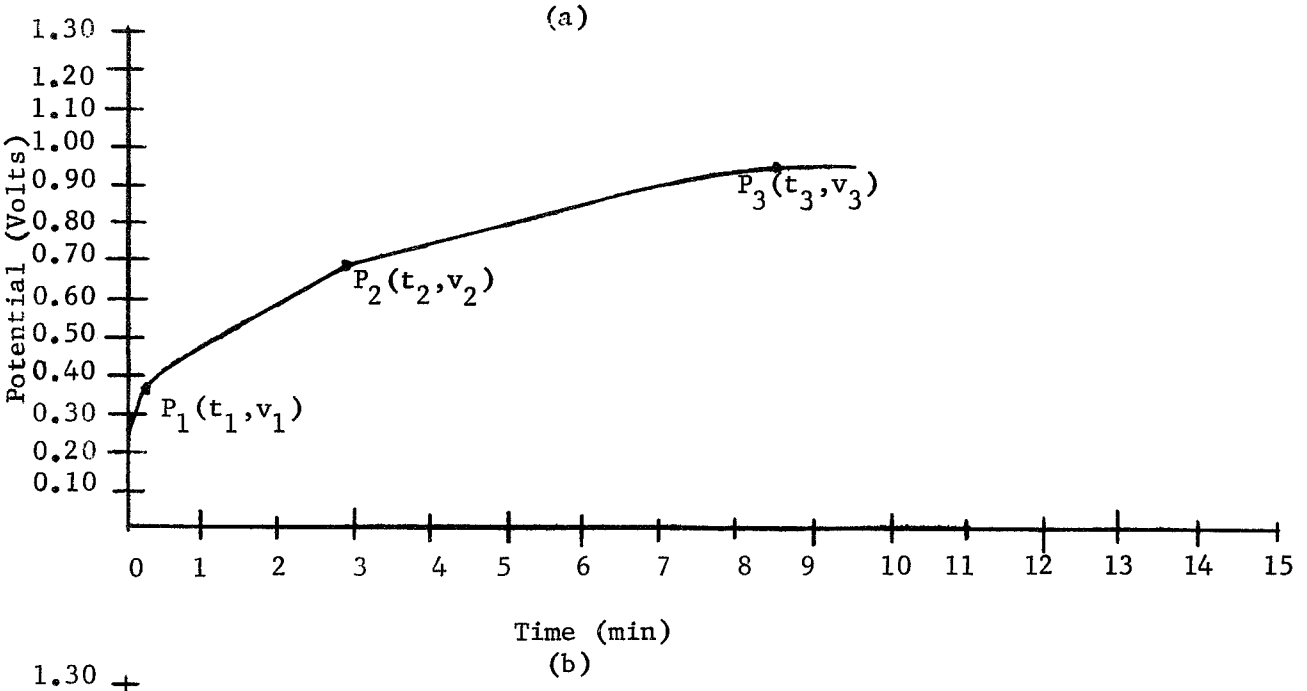

(b)

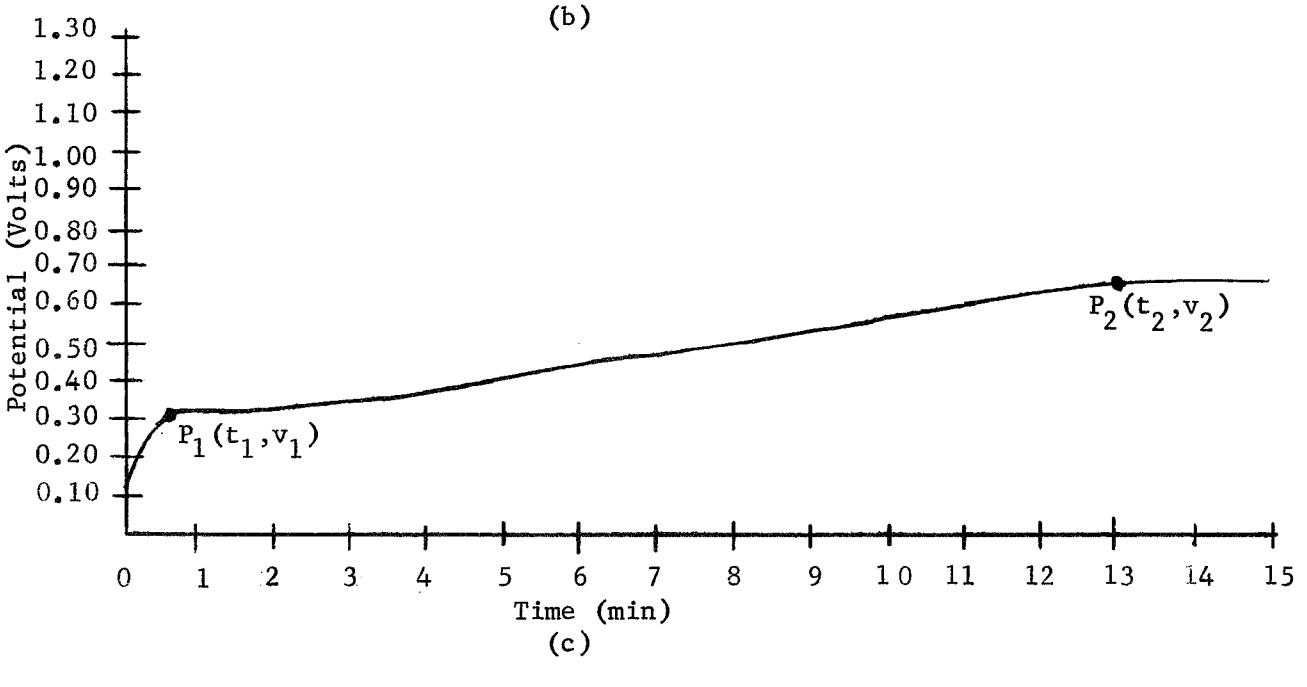

(c)

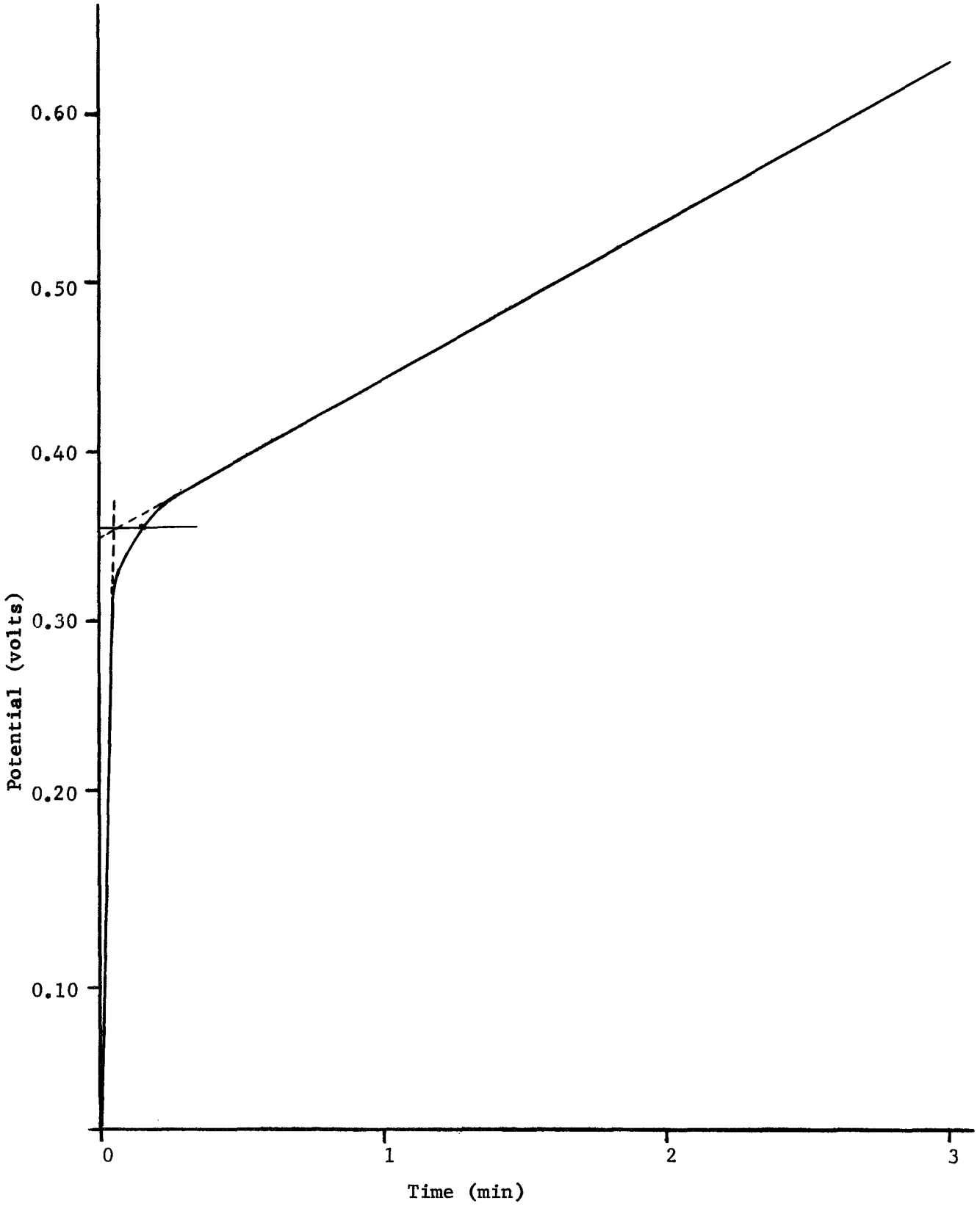

Fig. 4 -- Figure 3a (X6)

TABLE II

Oxidation Potentials for $P_1(t_1,v_1)$ and $P_2(t_2,v_2)$

at Various Currents

	POTENTIAL (VOLTS)									
	At 250 μa		At 500 μa		At 1100 μa		At 1600 μa		At 2000 μa	
ELECTRODE	$P_1(t_1,v_1)$	$P_2(t_2,v_2)$	$P_1(t_1,v_1)$	$P_2(t_2,v_2)$	$P_1(t_1,v_1)$	$P_2(t_2,v_2)$	$P_1(t_1,v_1)$	$P_2(t_2,v_2)$	$P_1(t_1,v_1)$	$P_2(t_2,v_2)$
B	0.31	0.66	0.36	0.72	0.55.	0.89				
B	0.31	0.66	0.36	0.72	0.54	0.89				
A			0.41	0.74	0.45	0.79	0.49	0.83	0.50	0.85
A			0.40	0.73	0.45	0.78	0.49	0.82	0.50	0.85
C	0.39	0.71	0.41	0.72	0.47	0.77	0.51	0.80		
C	0.39	0.70	0.41	0.72	0.46	0.78	0.50	0.80		

TABLE III

$t_2 - t_1$ for the Oxidations Recorded in Table II

	$t_2 - t_1$ (SEC)				
ELECTRODE	At 250 μa	At 500 μa	At 1100 μa	At 1600 μa	At 2000 μa
B	750	132	22		
B	742	168	26		
A		492	90	45	33
A		486	96	45	33
C	1200	270	36	15	
C	1200	258	36	17	

and 2000 μA, and for electrode C at 2000 μA because at these currents the potential rose very quickly to that of oxygen evolution with no sharp changes of slope. Bubbles appeared at the opening to the electrode in the first few seconds of oxidation in such size and quantity that they effectively shielded portions of the electrode from the counter electrode.

Table III shows the time intervals between P_1 and P_2 in the oxidations recorded in Table II. It can be seen that at 500 μA current, the time interval t_2-t_1 is longer for electrode B than for electrode A which has a larger surface area. This would be expected if the oxide formed during this period is a function of surface area only. Comparison of these times for electrodes A and C shows a substantial decrease even though electrode C has 30% more area than electrode A. Apparently the time of oxidation at constant current is not a function of area alone but also depends upon the pore size.

Electrode C has greater surface area than has A and this increase in area results from a larger number of smaller wires being used. The pores are smaller (inside pores, 0.99 mm^2 compared with 2.04 mm^2 for electrode A) and this smaller size has two results which can possibly affect the charge acceptance: (a) changes in the electrolyte flow characteristics; and (b) changes in the electrolyte resistance in the individual pore. The changes in flow characteristics will be eliminated by the use of a static electrolyte system (the flowing system was initially chosen to eliminate problems

of electrolyte depletion in very small pores). Experiments made with such a static system should demonstrate the effect of electrolyte resistance upon charge acceptance.

When a cleaned electrode is first cycled through oxidation and reduction it loses its metallic sheen and acquires a light grey dull finish that deepens to a medium grey with more cycling. The dull grey is thought to be finely divided silver, deposited during reduction. The presence of finely divided silver on the electrode would increase the surface area, and the data in Table IV demonstrate that this is the process occurring. The last three oxidations indicate that a constant maximum surface area is obtained, and this is substantiated by the stabilization of the electrode color at medium grey.

An interesting phenomenon was observed at P_2 in the oxidation of electrode C, and is illustrated in Figure 5. The voltage remained constant for a period of time, rose sharply to a new potential ($\Delta V \approx 0.01$ volt), remained constant for a period of time, and rose again giving the curve a step-like shape. The steps are just discernible at 1600 μA, more pronounced at 1100 μA, less definite but more numerous at 500 μA, and undetectable at 250 μA.

As shown above, each electrode has three pores of different shape and size. Both visual and microscopic examination failed to show preferential oxide growth in any one when compared to the other two.

Future work on these model pore electrodes will include exper-

TABLE IV

Oxidation of Freshly Cleaned Electrode

Electrode	Run Number	Potential (Volts) At $P_1(t_1,v_1)$	At $P_2(t_2,v_2)$
C	40	0.46	0.81
C	41	0.44	0.78
C	42	0.42	0.73
C	43	0.40	0.71
C	49	0.41	0.72
C	50	0.41	0.72

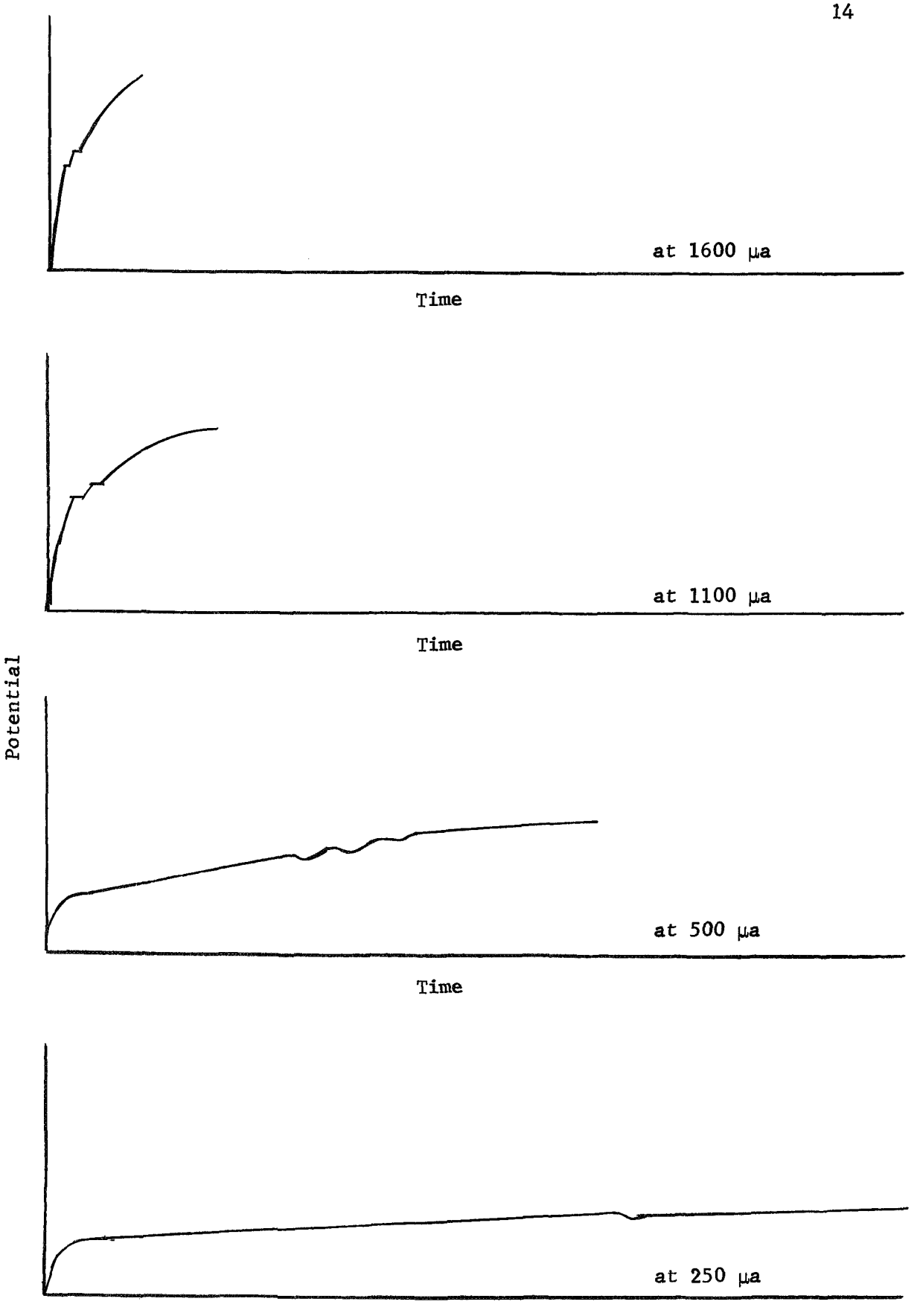

Fig. 5. Oxidation phenomena for electrode C

iments with the electrolyte held in a static condition during the oxidation and a detailed examination of electrolyte resistance as a function of pore size.

SECTION II

CHARGE ACCEPTANCE OF SILVER ELECTRODES

Introduction

In our approach to the determination of suitable methods for the estimation of the effective electrolytic surface area of silver electrodes we have used both constant current and potentiostatic oxidations of these electrodes. The need for a more detailed examination of the initial stages of oxidation under potentiostatic conditions is evident from the very rapid rise of current when a specific finite potential is imposed on an electrode. The mechanical response of the recorders we have been using is inadequate to record correctly the resultant current flow. Our initial efforts to examine this aspect of charge acceptance with an oscilloscope are reported here. The oscilloscope has a persistence feature which permits adequate visual observation of the initial current response in these potentiostatic oxidations.

An interesting feature of oxidations of silver electrodes under potentiostatic conditions is the apparent large dependence of charge acceptance upon the controlled potential. The plot of charge acceptance versus potential showed two distinct maxima;[2] one possible explanation of this is found in the observation of the formation of an initial basal layer of oxide.[3] If the characteristics of this basal layer are a function of the potential at which it is formed, then the extent of further oxidation at a constant potential could be significantly changed by changed values of that potential. This possibility also suggests the need to examine closely the initial stages of the

oxidation of silver under potentiostatic conditions.

Experimental

In Figure 6 is shown the cell design for oxidation under potentiostatic conditions and Figure 7 shows the circuit diagram. The electrolyte used was 0.1008 F KOH, and was replaced with new electrolyte at the beginning of each day's experimental work. The reference electrode was mercury-mercuric oxide. A cylinder of 0.003 inch thick platinum foil 4.7 cm in diameter and 2.5 cm high served as the counter electrode. The bottom edge of this cylinder reached just to the bottom of the cell chamber. In no case did the electrolyte level reach the top of the counter electrode. The cell and electrolyte were thermostatted at 20.0 ± 0.1°C during all experiments.

The electrodes were prepared from 0.010 inch silver wire which was scoured with an abrasive cleanser and rinsed thoroughly with distilled water just prior to use. The electrode was then placed in the cell, concentric with the platinum counter electrode, and with its lower end just at the bottom of the cell chamber. An electrode was used for a single oxidation and then replaced with a new electrode. The cell and electrode placement were designed to give uniform current distribution.

The length of the electrode which was oxidized was controlled by the depth of the electrolyte and was measured with a vernier caliper after the electrode had been removed. In the case of oxidations at the lowest potentials the oxide layer was so thin and difficult to

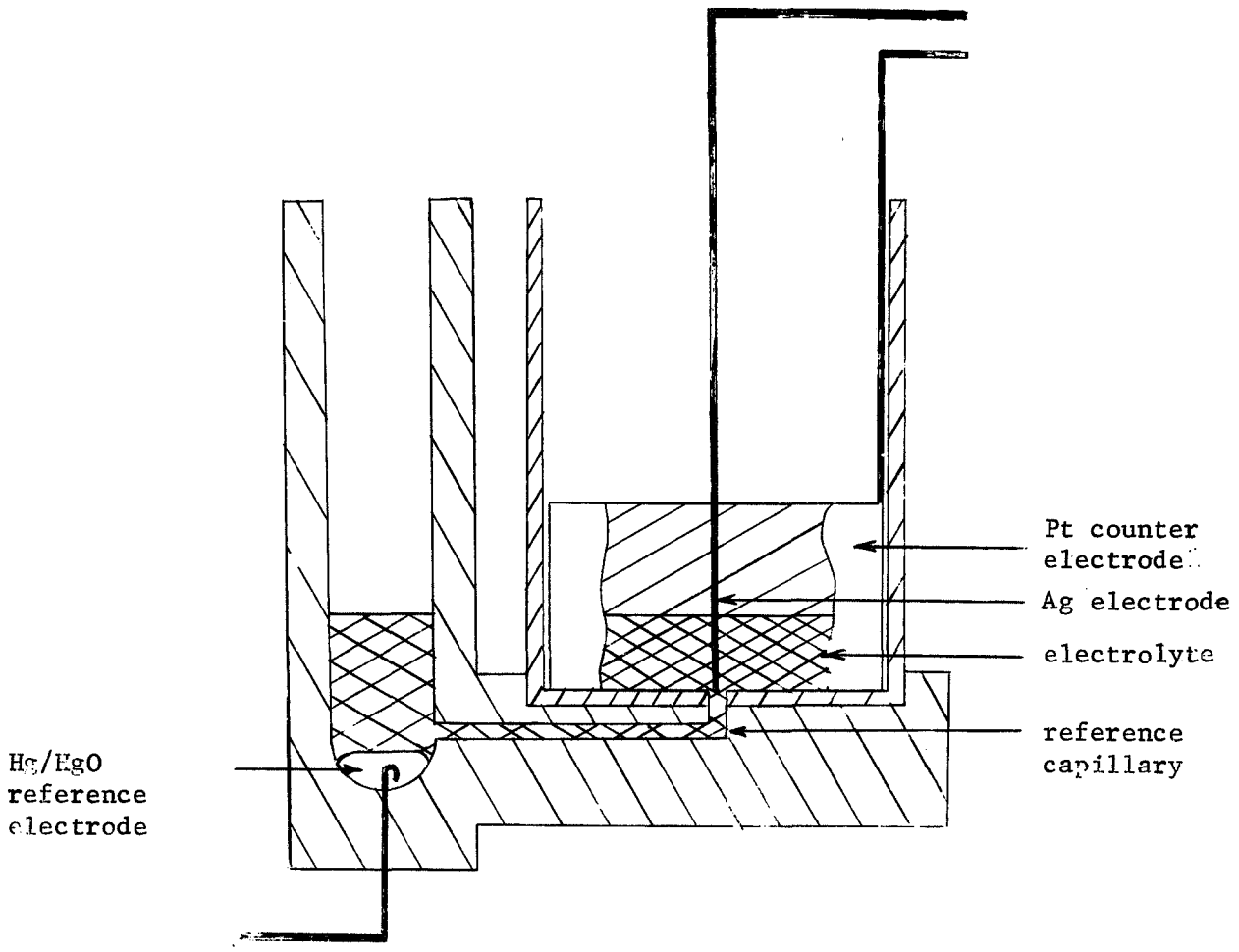

Fig. 6. -- Cross sectional view of cell used in study of current peak heights with view of positioning of silver electrode.

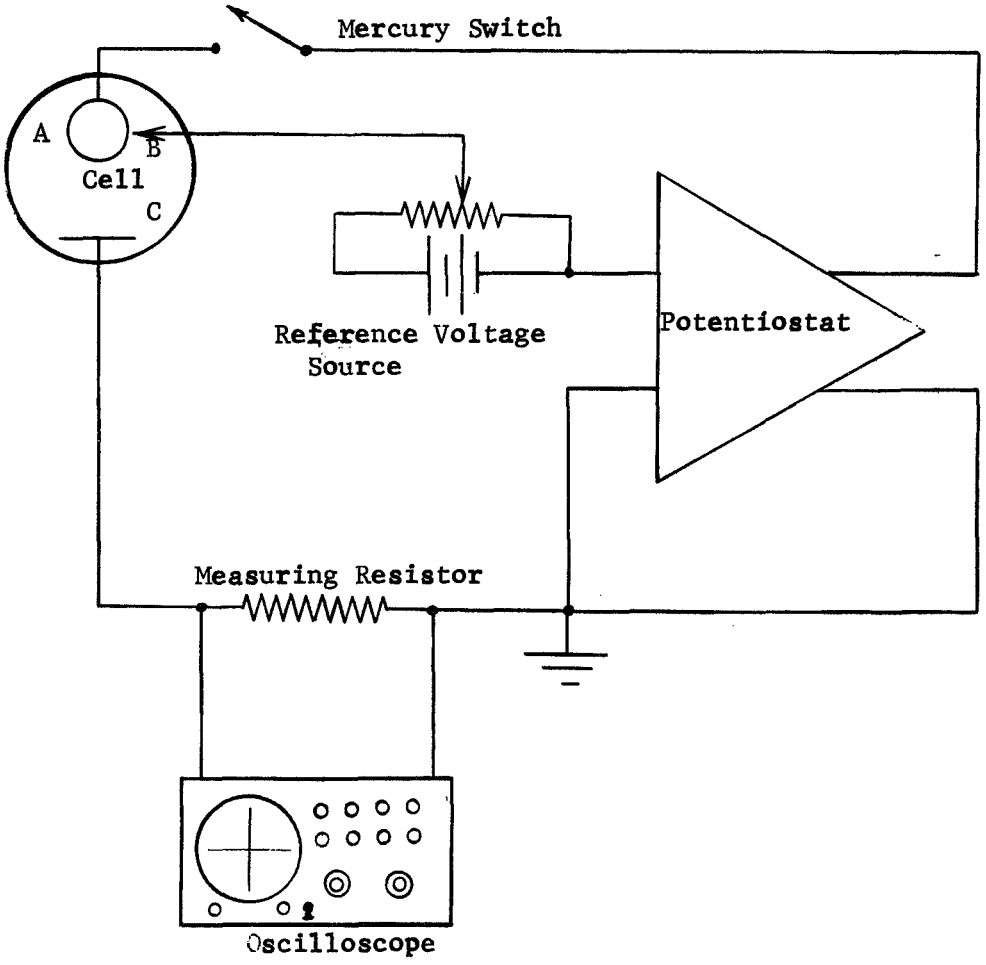

Fig. 7. --- Schematic diagram of cell, potentiostat, and oscilloscope. A is the anode, B is the reference electrode, and C is the counter electrode.

see that measurements of its length were uncertain; therefore, after experiments at such potential values an increased potential was imposed upon the electrode pair for a few seconds in order to make an easily measureable oxide coating.

All external wiring in the circuitry was shielded to prevent 60 Hz interference. Initially a toggle switch was used in the circuit represented in Figure 7, but this was replaced by a mercury switch because the current traces showed evidence of point-bounce in the switch. The change to the mercury switch removed this difficulty.

RESULTS AND DISCUSSION

A typical trace on the CRT of the oscilloscope is shown in Figure 8. The applied potential in this determination is 0.3500 volts. Within 0.20 millisecond the current density has increased to a peak value of 75 milliamps/cm^2. A decrease to half this value occurs within 2.0 milliseconds. The peak value of current density under similar conditions but with a strip chart recorder as previously observed[4] was never more than four milliamps/cm^2.

Data from 139 experimental runs at five fixed potentials are shown in Table V and are plotted in Figure 9. The standard deviation in the maximum current density at a given potential ranges from 13.3 ma/cm^2 at 0.300 volt vs Hg-HgO to 27.0 ma/cm^2 at 0.400 volt vs Hg-HgO. While the reproducibility is poor, the data do show an approximately linear character through the range of potentials covered. There is no evidence of the two maxima which

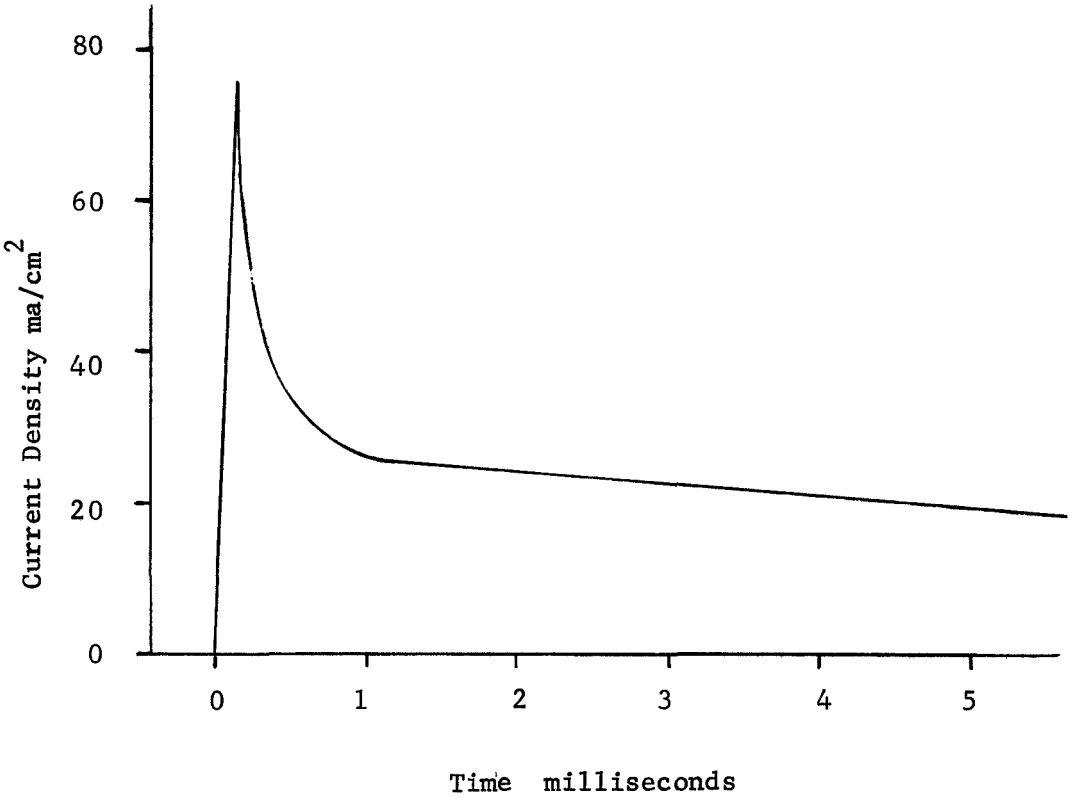

Fig. 8.-- A typical trace of peak current density as seen on oscilloscope. The anode potential is 0.3500 volt versus Hg/HgO reference electrode.

TABLE V

Initial Peak Values of Current Density of Silver Wire Electrodes Subjected to Fixed Controlled Potential

Potential Volts	Peak Values of Current Density ma/cm^2	Number of Runs	Standard Deviation ma/cm^2	% S.D.
0.3000 ± 0.0017	64.1	17	13.3	20.7
0.3500 ± 0.0011	77.1	18	15.5	20.1
0.4000 ± 0.0014	99.8	64	27.0	27.0
0.4750 ± 0.0004	121.1	13	18.2	15
0.5500 ± 0.0012	130.0	27	23.5	16.1

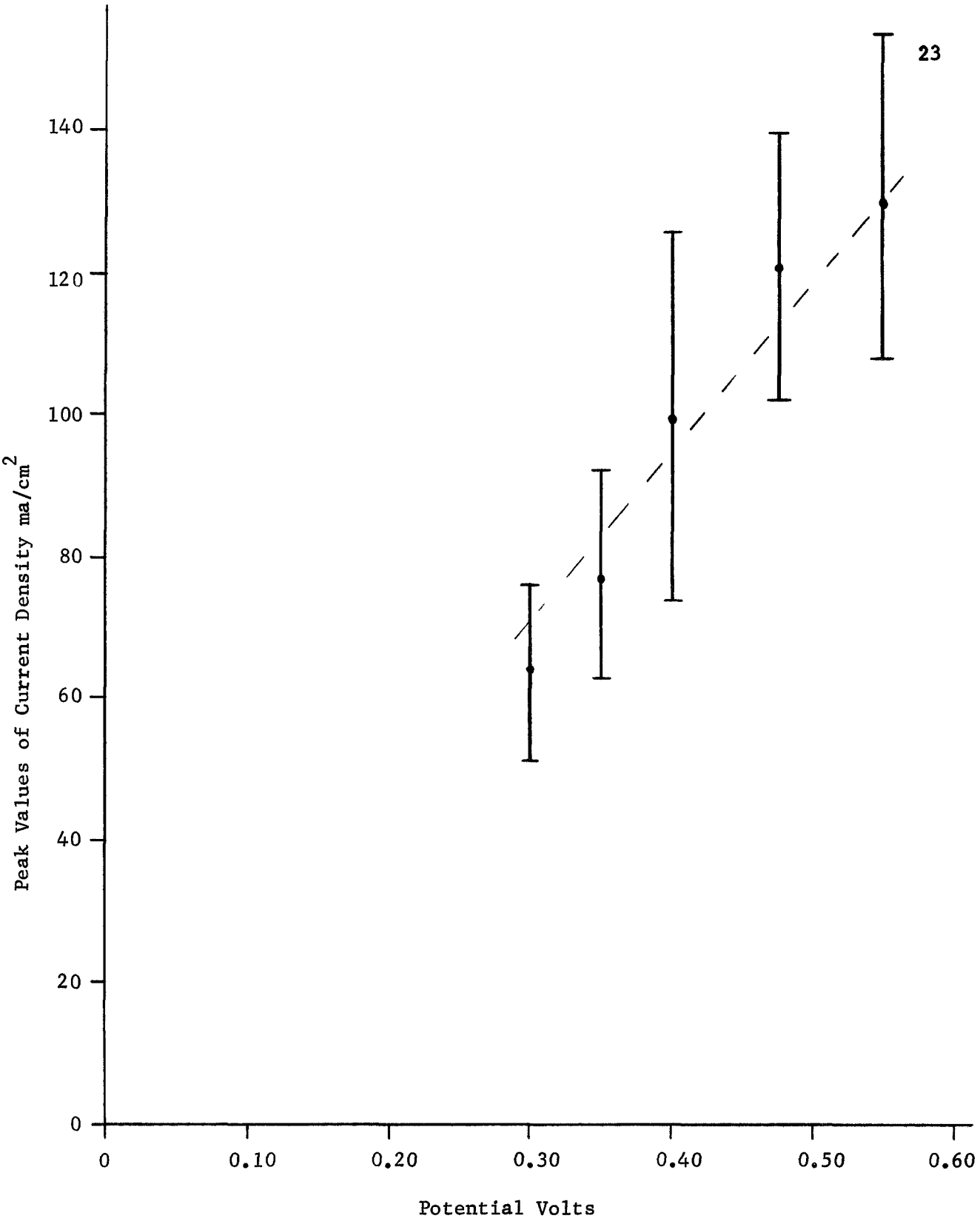

Fig. 9 -- Initial peak values of current density of silver wire electrodes subjected to fixed controlled potential.

were observed in the plot of charge acceptance versus the controlled potential.[2] Measurements were made through the range 0.30 volt to 0.55 volt vs Hg-HgO because this is the range of potentials in which oxidation to Ag_2O occurs. Calculations of the charge accepted by the time the initial current flow reaches its peak value show values ranging from 8.4×10^{-10} faraday/cm^2 at 0.30 volt to 17×10^{-10} faraday/cm^2 at 0.55 volt. This corresponds to one unit of charge per 20 and 10 square anstroms of surface respectively.

Based on a value of 300 μfd/cm^2 for the double layer capacitance of a silver electrode,[5] the charge accepted in charging the double layer is 9.4×10^{-10} faraday/cm^2. This corresponds to one unit of charge per 18 square angstroms of surface.

A comparison of these calculations suggests that the current flow until the peak value is reached could be accounted for by charging of the double layer.

The discussion of Fleischmann, Lax, and Thirsk[3] on the charge acceptance of silver electrodes includes the postulation of a basal layer of argentous oxide which covers the surface and which influences further deposition of argentous oxide and still later argentic oxide.

Our interest in the initial peak values of current density was based on the supposition that these peak values would be related to the characteristics of the basal layer. If, however, the initial peak values result only from the charging of the double layer, which occurs in less than one millisecond, oxidation over

a longer time span, i.e. 1-1000 milliseconds, should be examined for possible relationships of charge acceptance to characteristics of the basal layer. Such experiments will be performed during the next quarter.

Also, if the initial peak values of current density result only from charging of the double layer, we should observe similar peak values at potentials less than 0.30 volt. These experiments will be performed also.

REFERENCES

1. E. A. Butler and A. U. Blackham, "Studies of Reaction Geometry in Oxidation and Reduction of the Alkaline Silver Electrode", Fifth Quarterly Report, J. P. L. 952268, August 15, 1969.

2. Figure 6 - Reference 1.

3. M. Fleischmann, P. J. Lax, H. R. Thirsk, Trans. Faraday Soc., 64, 3128 (1968).

4. Figure 6 - E. A. Butler and A. U. Blackham, "Studies of Reaction Geometry in Oxidation and Reduction of the Alkaline Silver Electrode", Third Quarterly Report, J. P. L. 952268, February 15, 1969.

5. B. D. Cahan, J. B. Ockerman, R. F. Amlie, and P. Ruetschi, J. Electrochem. Soc., 107, 725 (1960).